Nodal Signaling Regulates Germ Cell Development and Establishment of Seminiferous Cords in the Human Fetal Testis

Article

Cell Reports

Nodal Signaling Regulates Germ Cell Development and Establishment of Seminiferous Cords in the Human Fetal Testis

Graphical Abstract

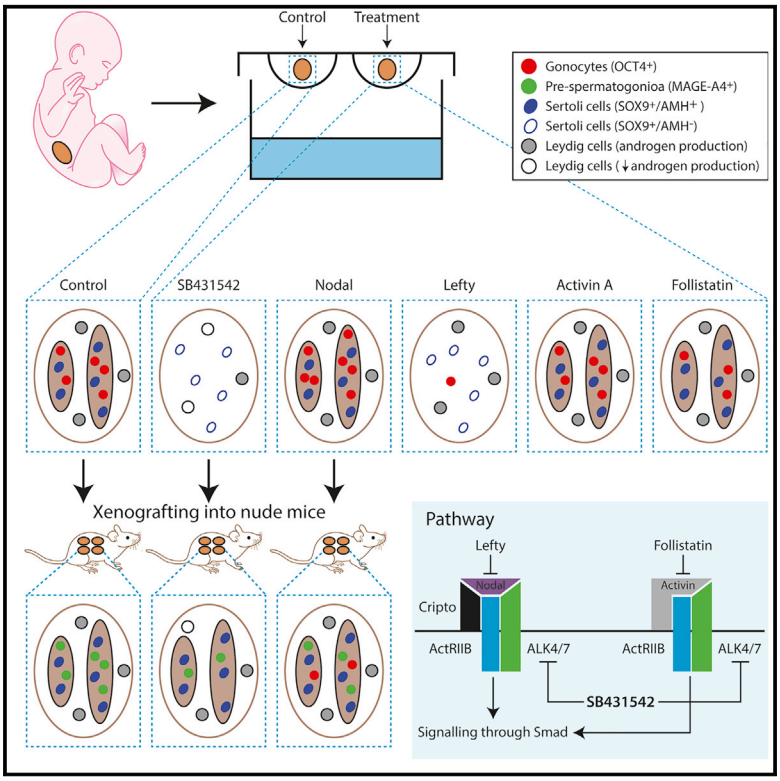

Highlights

- Nodal and Activin signaling was manipulated during human testicular development
- Inhibiting Nodal/Activin signaling results in testicular dysgenesis and gonocyte loss
- Effects on somatic cell lineages and testicular morphology are rescued with time
- Nodal pathway stimulation results in persisting gonocytes resembling TGCC precursors

Authors

Anne Jørgensen, Joni Macdonald, John E. Nielsen, ..., Richard M. Sharpe, Ewa Rajpert-De Meyts, Rod T. Mitchell

Correspondence

aj@rh.regionh.dk

In Brief

Jørgensen et al. determine the role of Nodal signaling in human fetal testis development using *ex vivo* culture and xenografting approaches. They provide insights into the involvement of Nodal signaling in seminiferous cord formation and the regulation of pluripotency factor expression in fetal gonocytes, with implications for the development of testicular cancer.

Jørgensen et al., 2018, Cell Reports *25*, 1924–1937
November 13, 2018
https://doi.org/10.1016/j.celrep.2018.10.064

CellPress

OPEN ACCESS
CellPress

Cell Reports
Article

Nodal Signaling Regulates Germ Cell Development and Establishment of Seminiferous Cords in the Human Fetal Testis

Anne Jørgensen,[1,2,7,*] Joni Macdonald,[3] John E. Nielsen,[1,2] Karen R. Kilcoyne,[3] Signe Perlman,[4] Lene Lundvall,[4] Lea Langhoff Thuesen,[5] Kristine Juul Hare,[5] Hanne Frederiksen,[1,2] Anna-Maria Andersson,[1,2] Niels E. Skakkebæk,[1,2] Anders Juul,[1,2] Richard M. Sharpe,[3] Ewa Rajpert-De Meyts,[1,2,6] and Rod T. Mitchell[3,6]

[1]Department of Growth and Reproduction, Rigshospitalet, University of Copenhagen, Blegdamsvej 9, 2100 Copenhagen, Denmark
[2]International Research and Research Training Centre in Endocrine Disruption of Male Reproduction and Child Health (EDMaRC), Blegdamsvej 9, 2100 Copenhagen, Denmark
[3]MRC Centre for Reproductive Health, The Queen's Medical Research Institute, University of Edinburgh, 47 Little France Crescent, Edinburgh EH16 4TJ, UK
[4]Department of Gynaecology, Rigshospitalet, University of Copenhagen, Blegdamsvej 9, 2100 Copenhagen, Denmark
[5]Department of Obstetrics and Gynaecology, Hvidovre University Hospital, Kettegård Alle 30, Hvidovre, Denmark
[6]These authors contributed equally
[7]Lead Contact
*Correspondence: aj@rh.regionh.dk
https://doi.org/10.1016/j.celrep.2018.10.064

SUMMARY

Disruption of human fetal testis development is widely accepted to underlie testicular germ cell cancer (TGCC) origin and additional disorders within testicular dysgenesis syndrome (TDS). However, the mechanisms for the development of testicular dysgenesis in humans are unclear. We used *ex vivo* culture and xenograft approaches to investigate the importance of Nodal and Activin signaling in human fetal testis development. Inhibition of Nodal, and to some extent Activin, signaling disrupted seminiferous cord formation, abolished AMH expression, reduced androgen secretion, and decreased gonocyte numbers. Subsequent xenografting of testicular tissue rescued the disruptive effects on seminiferous cords and somatic cells but not germ cell effects. Stimulation of Nodal signaling increased the number of germ cells expressing pluripotency factors, and these persisted after xenografting. Our findings suggest a key role for Nodal signaling in the regulation of gonocyte differentiation and early human testis development with implications for the understanding of TGCC and TDS origin.

INTRODUCTION

Sex-specific differentiation of bipotential fetal gonads involves a complex interplay of signaling cascades, which direct cell lineage specification and establishment of the somatic cell niche appropriate for testis or ovary development (Rotgers et al., 2018). The differentiation of germ cells in both sexes is directed by cues from the somatic cells that trigger differentiation in either the male or female direction, resulting ultimately in spermatogenesis or oogenesis. The regulation of somatic cell differentiation and commitment of the germ cell lineage in the human fetal testis is not well understood. There are many similarities, but also clear differences compared to mice, from which the majority of the current knowledge on mammalian early gonad development has been established. Human testis differentiation is initiated around gestational week (GW) 6, when the primordial germ cells have arrived in the bipotential gonad and become surrounded by somatic precursor cells. Expression of SRY and SOX9 is initiated, resulting in the differentiation of Sertoli cells and enclosing of germ cells (at this stage called gonocytes) within seminiferous cords (Sinclair et al., 1990; Berta et al., 1990; Hanley et al., 2000). The organization of seminiferous cords is initiated at approximately GWs 7–8, with cords clearly present from GWs 9–10. The interstitial cell populations, including fetal Leydig cells, progenitors of adult Leydig cells, and progenitors of peritubular myoid cells are also established at the same time (Ostrer et al., 2007). The somatic cell niche in the fetal testes is organized to ensure optimal support of the germ cells, including at this early developmental time point a high proliferation rate of gonocytes (Bendsen et al., 2003) and prevention of gonocytes entering meiosis (Jørgensen and Rajpert-De Meyts, 2014).

Gonocytes in the human fetal testis are characterized by the expression of pluripotency factors, including OCT4, NANOG, and AP2γ, which are gradually downregulated in an asynchronous manner, starting at approximately GWs 16–20, thereby marking the transition from gonocyte to pre-spermatogonium (Jørgensen et al., 1995; Hoei-Hansen et al., 2004; Gaskell et al., 2004; Rajpert-De Meyts et al., 2004; Honecker et al., 2004; Pauls et al., 2006; Mitchell et al., 2008). The pre-spermatogonial population can be distinguished from gonocytes by the expression of MAGE-A4, distinct morphology, and their localization closer to the basement membrane within the seminiferous tubule compared to gonocytes (Rajpert-de Meyts and Hoei-Hansen, 2007). This transition from germ cells expressing pluripotency factors to a more differentiated phenotype is a key event in normal

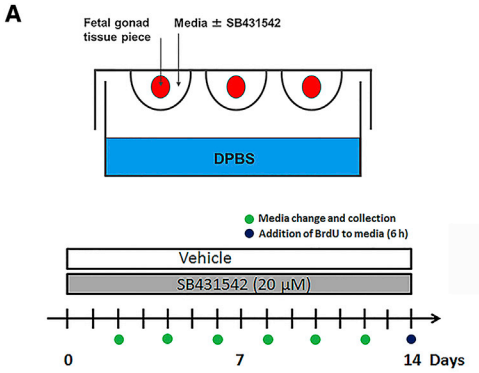

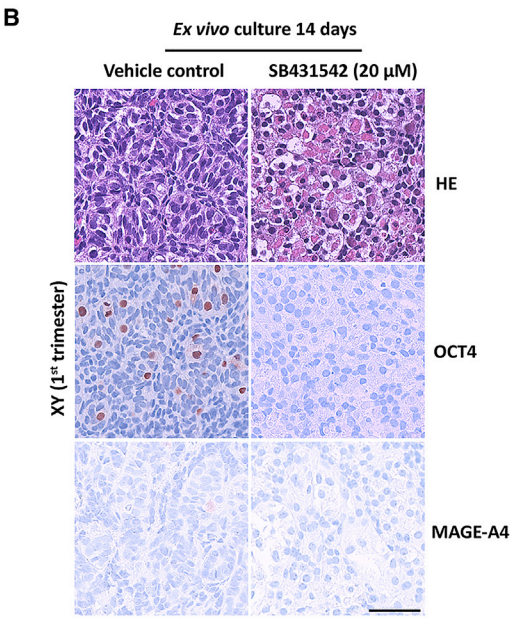

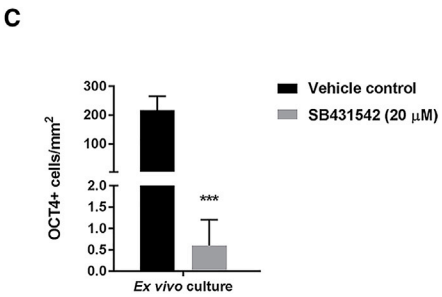

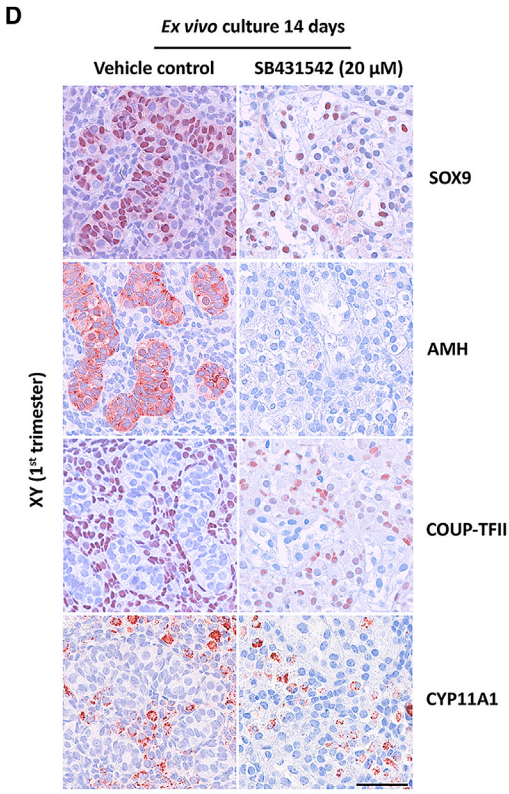

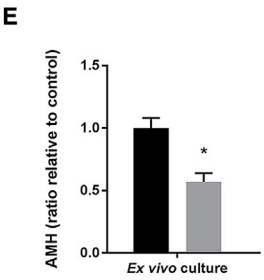

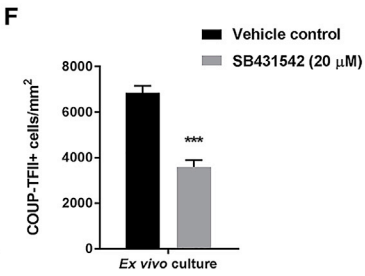

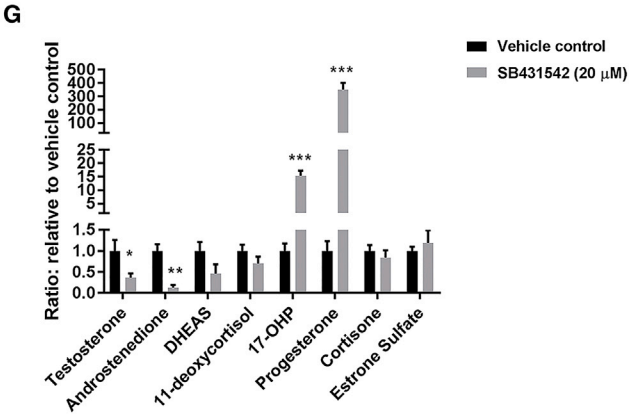

(legend on next page)

perinatal testis development, and the disruption of this transition may have consequences later in life. Premature germ cell differentiation may result in germ cell loss, with potential effects on fertility in adult life, while failure to differentiate can result in an arrested gonocyte population, which develops into testicular germ cell cancer precursor cells, called germ cell neoplasia *in situ* (GCNIS, previously known as carcinoma *in situ*). GCNIS cells develop into malignant testicular germ cell tumors in young adulthood (Skakkebaek et al., 2016; Rajpert-De Meyts et al., 2016).

The molecular mechanisms directing the transition from gonocyte to pre-spermatogonium are currently not characterized in detail in humans, but recent studies in mice have demonstrated a role for Nodal and Activin signaling in the regulation of pluripotency factor expression in early embryonic germ cell differentiation (Souquet et al., 2012; Spiller et al., 2012; Wu et al., 2013; Miles et al., 2013). Nodal and Activin both signal through binding to a receptor complex consisting of ActRII and ALK4/7, with Nodal also requiring the presence of the co-receptor Cripto. Binding and activation of these receptor complexes lead to the phosphorylation of Smad2/3, which regulates the transcription of target genes that for Nodal signaling includes *Nodal* itself, as well as its endogenous inhibitor *Lefty* (Papanayotou and Collignon, 2014; Spiller et al., 2017). Activation of SMAD2/3 via transforming growth factor β (TGF-β), Activin or Nodal signaling is necessary for the maintenance of pluripotency in human embryonic stem cells (James et al., 2005), which implicates these pathways as possible regulators of the expression of pluripotency factors in human fetal gonocytes. Nodal and Activin signaling have also been implicated in the prevention of premature meiotic entry of germ cells in mice (Souquet et al., 2012; Wu et al., 2013; Miles et al., 2013) and in the formation of testicular cords during mouse testis differentiation (Wu et al., 2013; Miles et al., 2013). Because the occurrence of GCNIS cells in humans often coincides with focal testicular dysgenesis (Hoei-Hansen et al., 2003), it raises the possibility of a role for Nodal and/or Activin dysfunction in the origin of testicular dysgenesis syndrome (TDS). Testicular dysgenesis syndrome comprises a group of disorders that include GCNIS, testicular germ cell cancer, cryptorchidism, and some forms of hypospadias and infertility, which result from abnormal fetal testis development (Skakkebaek et al., 2001, 2016). In this study, we sought to investigate the role of Nodal and Activin signaling in human fetal testis development by examining the consequences of experimentally manipulating these signaling pathways at different developmental time points. Our study demonstrates that the Nodal pathway plays a key role in the regulation of pluripotency factor expression in human gonocytes and in the establishment of the seminiferous cords. In addition to the distinct Nodal-mediated events in human testicular development, there are overlapping roles of Nodal signaling and Activin signaling involved in mediating normal human fetal testis development, including anti-Müllerian hormone (AMH) secretion, fetal germ cell survival, and steroidogenesis.

RESULTS

Nodal and Activin Signaling Factors Are Expressed in Human Fetal Testis

To establish the presence and expression level of key factors in the Nodal and Activin signaling pathways in human fetal testis, qPCR was conducted. Testis samples from the first and second trimesters and ovary samples from the first trimester were included in the analysis. All of the investigated factors (*ALK4*, *ALK5*, *ALK7*, *ACVR2B*, *NODAL*, *CRIPTO*, *LEFTY*, *INHBA*, *INHBB*) involved in Nodal and Activin signaling were expressed in human fetal testis and ovary samples from the first trimester and in testis samples from the second trimester, each with a distinct expression pattern (Figure S1). The only exception was *ALK7,* which was detectable in only 3 of 40 investigated samples. The observed expression pattern is consistent with both Nodal and Activin signaling playing a role in human fetal testis development.

Effects of SB431542 Exposure on Germ Cells in Human First Trimester Testis Cultures

To examine the role of Nodal and Activin signaling in fetal testis development, isolated first trimester fetal testis tissue was cultured in the presence of the specific ALK4/5/7 inhibitor SB431542 for 2 weeks (Figure 1A). This simultaneous inhibition of Nodal signaling and Activin signaling resulted in the

Figure 1. Effects of Simultaneous Inhibition of Nodal and Activin Signaling in First Trimester Human Fetal Testis *Ex Vivo* Culture on Overall Morphology, Germ Cell Number, and Somatic Cell Function

(A) Experimental overview of SB431542 (ALK4/5/7 inhibitor) treatment resulting in the simultaneous inhibition of Nodal and Activin signaling pathways in human fetal testis samples from first trimester during 14 days of culture. DPBS, Dulbecco's PBS.

(B) Morphology and expression pattern of germ cell markers OCT4 (gonocytes) and MAGE-A4 (pre-spermatogonia) in fetal testis samples treated with SB431542 (20 μM) for 2 weeks in *ex vivo* culture. Tissue from nine fetuses was investigated. Counterstaining with Mayer's hematoxylin; scale bar corresponds to 50 μm.

(C) Quantification of germ cells determined as the number of $OCT4^+$ gonocytes per square millimeter. Values represent means ± SEMs, with n = 9. Significant difference compared to vehicle control, ***$p < 0.001$.

(D) Expression pattern of somatic cell markers, including SOX9 and AMH (Sertoli cells), COUP-TFII (interstitial cells), and CYP11A1 (fetal Leydig cells). Tissue from nine fetuses was investigated. Counterstaining with Mayer's hematoxylin; scale bar corresponds to 50 μm.

(E) Quantification of AMH produced by the fetal testis in *ex vivo* culture and secreted into the media. Medium was collected every 48 hr throughout the 14-day culture period and was pooled for each individual tissue piece. AMH was measured by ELISA and is shown as the ratio compared to vehicle controls. Values represent means ± SEMs, with n = 7. Significant difference compared to vehicle control, *$p < 0.05$.

(F) Quantification of COUP-TFII positive cells per square millimeter. Values represent means ± SEMs, with n = 7. Significant difference compared to vehicle control, ***$p < 0.001$.

(G) Quantification of androgens produced in the fetal testis *ex vivo* cultures and secreted to the media droplets. Media was collected every 48 hr throughout the 14-day culture period and was pooled for each individual tissue piece. Androgens were measured by liquid chromatography-tandem mass spectrometry (LC-MS/MS) and are shown as ratios compared to corresponding vehicle controls. Values represent means ± SEMs, with n = 7. Significant difference compared to vehicle control, *$p < 0.05$, **$p < 0.01$, and ***$p < 0.001$.

near-complete loss of OCT4$^+$ gonocytes in fetal testes explants (Figure 1B), as confirmed by their quantification ($p < 0.001$; Figure 1C). To determine whether this was due to specific downregulation of OCT4 or a general downregulation of pluripotency factors, the expression of additional pluripotency-related proteins was investigated, including NANOG, AP2γ, SALL4, LIN28, and C-KIT. None of these additional pluripotency factors was expressed (except in a few cells, data not shown) in fetal testes samples cultured with SB431542, thus resembling the finding for OCT4. These observations did not distinguish whether SB431542 treatment resulted in the specific downregulation of pluripotency factors, premature differentiation of germ cells (with a resulting downregulation of pluripotency factors), or loss of the gonocyte population due to apoptosis or reduced proliferation. We ruled out the possibility that SB431542 treatment accelerated gonocyte differentiation by showing that only very few germ cells expressing MAGE-A4 (marker of pre-spermatogonia) were present in fetal testes cultures (Figure 1B). The lack of accelerated gonocyte differentiation was confirmed by the observation that no VASA$^+$ cells could be detected in fetal testes treated with SB431542, and no indication of SB431542-mediated premature initiation of meiosis was found based on the lack of SCP3$^+$ cells (Figure S2A). However, it is not possible to completely exclude that pluripotency factors are downregulated by SB431542 exposure as the first step in differentiation, without upregulation of MAGE-A4; as such, an OCT4$^-$/MAGE-A4$^-$ subpopulation of germ cells has been described previously (Gaskell et al., 2004).

All cell types in the fetal testis cultures continued proliferation in both vehicle- and SB431542-treated samples, as assessed by the incorporation of bromodeoxyuridine (BrdU) at the end of the culture period (14 days) and after 7 days of culture (Figure S3A). The number of proliferating (BrdU$^+$) gonocytes per square millimeter was significantly ($p < 0.001$) reduced in SB431542-treated fetal testis compared to vehicle controls (Figure S3B), which is in line with the overall reduced number of gonocytes (OCT4$^+$) detected in these samples (Figure 1C). Only a few apoptotic (cleavage product of poly-ADP-ribose polymerase-positive [cPARP$^+$]) cells were detected after 7 and 14 days of culture, regardless of treatment (Figure S3A); despite this, a significantly higher number of cPARP$^+$ cells per square millimeter were found after 14 days of culture in samples treated with SB431542 (Figure S3B). The observation of increased apoptosis in SB431542-treated fetal testes was confirmed by terminal deoxynucleotidyl transferase deoxyuridine triphosphate nick end labeling (TUNEL) staining, with more TUNEL$^+$ cells detected after both 7 and 14 days of culture (Figure S3A). These findings suggest that the reduction in gonocyte numbers in SB431542-treated fetal testis samples was the combined result of reduced proliferation and increased apoptosis during the culture period resulting from the simultaneous inhibition of Nodal and Activin signaling.

Effects of SB431542 Exposure on Somatic Cell Function in Human First Trimester Testis Cultures

To evaluate the effects of SB431542 treatment on somatic cell function, the histology of cultured first trimester fetal testes was evaluated, and a panel of immunohistochemical markers was used to evaluate key aspects of somatic cell function. The most pronounced effect of SB431542 treatment was that it disrupted normal seminiferous cord structure (Figure 1D), which was in contrast to the cultured vehicle control samples that showed normal fetal testis morphology (Figure 1D). Sertoli cells were clearly present in the SB431542-treated samples based on the expression of SOX9. However, their normal expression of AMH was completely abolished at the end of the culture period (Figure 1D). This observation was confirmed by the quantification of AMH secreted into the media during the 14-day culture period, which was significantly reduced ($p < 0.05$) in fetal testis cultures treated with SB431542 compared to vehicle controls (Figure 1E). This indicates that the Sertoli cells were affected either directly by the SB431542 treatment, indirectly by the reduced number of germ cells present, or through the disruption of the seminiferous cord structure. To determine whether the Sertoli cells had transdifferentiated toward a female granulosa-like cell type, the expression of FOXL2 was examined, but no positive cells were detected in either SB431542- or vehicle-treated fetal testis samples (Figure S2B). In the interstitial compartment, cells expressing chicken ovalbumin upstream promoter-transcription factor II (COUP-TFII) (mesenchymal and adult Leydig cells progenitors) and CYP11A1 (fetal Leydig cells) immunopositive cells were present in SB431542-exposed cultures, but the number of especially COUP-TFII$^+$ cells appeared to be reduced when compared to vehicle control samples (Figure 1D). This observation was confirmed after quantification, wherein a significantly lower ($p < 0.001$) number of COUP-TFII$^+$ cells per square millimeter were found in SB431542-treated samples (Figure 1F). In view of these observations, we evaluated whether fetal Leydig cells in SB431542-exposed testis cultures had altered steroidogenic function. Analysis of media from *ex vivo* cultures revealed that the secretion of testosterone and androstenedione were significantly reduced ($p < 0.05$ and $p < 0.01$, respectively) following SB431542 exposure (Figure 1G). In contrast, the level of early precursors in the steroidogenic pathway, namely 17-hydroxyprogesterone and progesterone were significantly ($p < 0.001$) elevated in SB431542-exposed samples compared to vehicle controls (Figure 1G), indicating treatment-related inhibition of CYP17A1 activity. These results suggest that the simultaneous inhibition of Nodal and Activin signaling in first trimester fetal testes disrupts seminiferous cord structure and impairs the normal function of both Sertoli and Leydig cells, the two key somatic cell types in the fetal testis.

Long-Term Effects of SB431542 Exposure in First Trimester Fetal Testes

To examine whether the adverse effects of SB431542 treatment in culture were permanent or recoverable, we cultured first trimester fetal testes for 6 days ±SB431542 and then xenografted the cultured tissue into castrated nude mice for 6 weeks without any additional treatment (Figure 2A). Following the 6-week grafting period, the majority of the effects observed after 6 days of SB431542 treatment appeared to have been rescued, except for the SB431542-induced loss of OCT4$^+$ gonocytes, because their numbers were significantly ($p < 0.05$) reduced both after 6 days' culture and after xenografting (Figures 2B and 2C). The seminiferous cords and the interstitial compartment appeared grossly normal after grafting of fetal testis tissue that

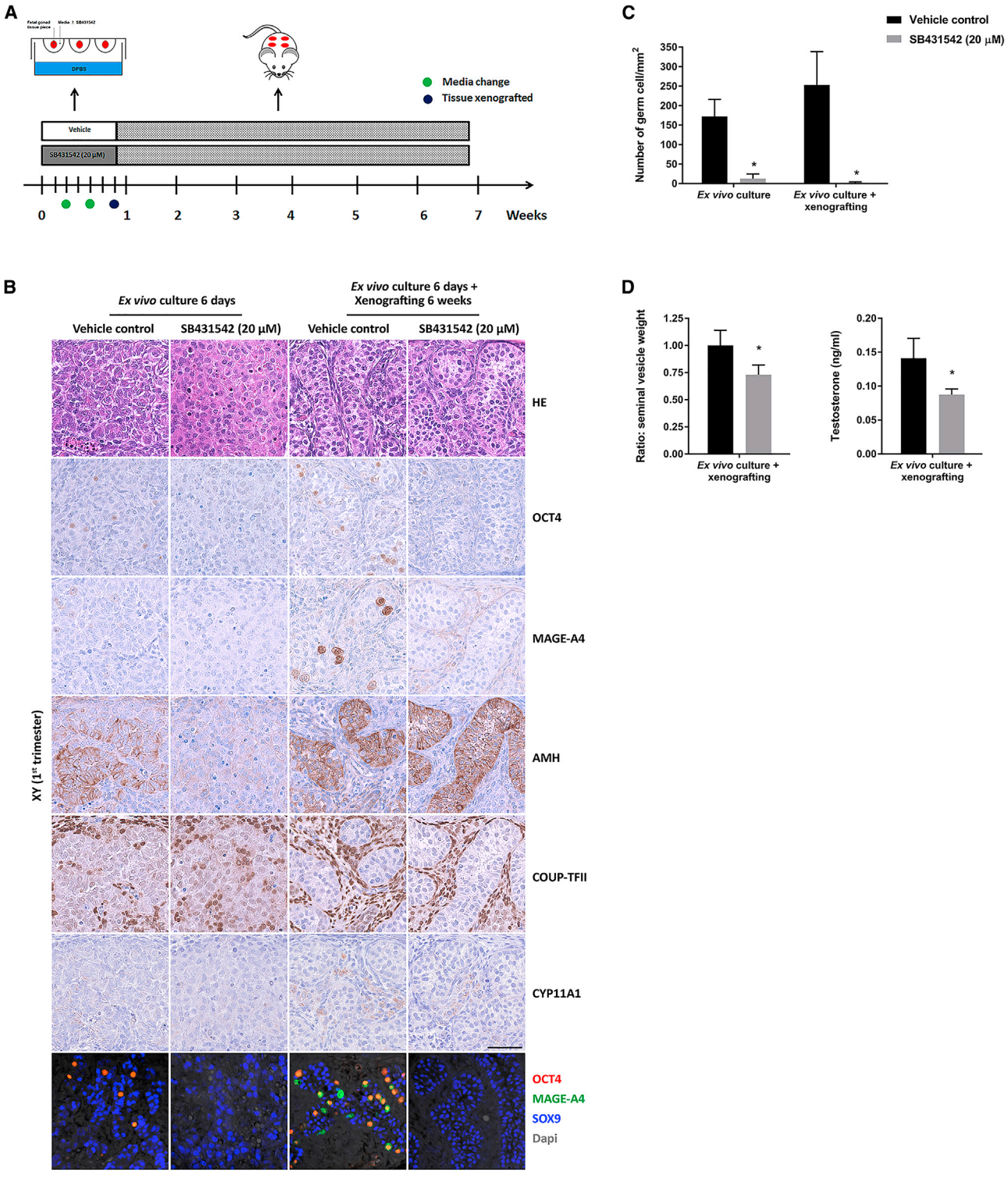

Figure 2. Long-Term Effects of Simultaneous Inhibition of Nodal and Activin Signaling in Human Fetal Testes from the First Trimester

(A) Experimental overview of treatment with SB431542 for 6 days in *ex vivo* culture, followed by xenografting for 6 weeks (without treatment).

(B) Effects of initial short-term treatment with SB431542 (20 μM) followed by xenografting on tissue morphology and expression of germ cell and somatic cell markers in first trimester fetal testis samples. Cultured and grafted samples (±SB431542) are compared to samples from the same fetus, which has only been cultured *ex vivo* (±SB431542). Immunohistochemical staining include OCT4 and MAGE-A4 (germ cell markers), AMH (Sertoli cell marker), COUP-TFII (marker of

(legend continued on next page)

had been initially exposed to SB431542 in culture. Moreover, the expression level and pattern of AMH, COUP-TFII, and CYP11A1 were unaltered compared to the corresponding vehicle control group following xenografting (Figure 2B). However, the initial SB431542 exposure in *ex vivo* culture exerted long-term effects on Leydig cell steroidogenesis, as shown by a significant ($p < 0.05$) decrease in host mouse seminal vesicle weight (in castrated mice, this is a readout of testosterone production from the xenografted tissue during the grafting period) and the significant ($p < 0.05$) reduction in serum testosterone levels in host mice (Figure 2D).

Long-Term Effects of SB431542 Exposure in Second Trimester Fetal Testes

To investigate whether SB431542 treatment of second trimester fetal testes in *ex vivo* culture resulted in effects resembling those observed in first trimester samples, a similar experimental setup was used with 6 days' SB431542 exposure in culture, followed by grafting of tissue pieces for 6 weeks (Figure 2A). In second trimester fetal testis samples, the germ cell population is a mixture of gonocytes ($OCT4^+$) and pre-spermatogonia ($MAGE\text{-}A4^+$). Following SB431542 exposure for 6 days in *ex vivo* culture, the number of gonocytes was severely reduced ($p < 0.05$) (Figures 3A and 3B). Furthermore, morphological evaluation revealed that a subpopulation of the pre-spermatogonia appeared abnormal (multinucleated) (Figures 3A and S4). Quantification of the number of pre-spermatogonia showed a significant reduction ($p < 0.05$) after the xenografting period in samples initially treated with SB431542. Also, the total number of germ cells per area ($OCT4^+$ + $MAGE\text{-}A4^+$) was significantly reduced ($p < 0.05$) after SB431542 exposure in *ex vivo* culture and an even larger reduction in numbers was observed following the xenografting period (Figure 3B). These results suggest that simultaneous SB431542-mediated inhibition of Nodal signaling and Activin signaling severely reduces the number of germ cells in second trimester fetal testes, with effects on both gonocyte and pre-spermatogonia populations.

The effects of SB431542 treatment on somatic cell function in second trimester testes were less evident compared to first trimester fetal testis tissue. After 6 days' exposure of second trimester fetal testes to SB431542, the seminiferous cord structure appeared normal, as did the expression of Sertoli cell markers AMH and SOX9 (Figure 3A). In contrast, both Leydig cells and peritubular myoid cells were affected, with only a few $CYP11A1^+$ Leydig cells evidently present in the interstitium, and an apparent loss of morphologically distinct peritubular myoid cells was observed (Figure 3A). After grafting of the tissue for 6 weeks, the Leydig cells (based on CYP11A1 expression) and the peritubular myoid cells (based on COUP-TFII expression) appeared similar between the initially SB431542- and vehicle-exposed samples (Figure 3A). In keeping with the normal expression of CYP11A1 after the xenografting period, there was no difference in the level of serum testosterone at the end of the grafting period between mice xenografted with SB431542- and vehicle-exposed testis tissue (Figure 3C). However, significantly lower seminal vesicle weight was found in mice grafted with testis tissue initially exposed to SB431542, implying that testosterone production during the grafting period may have initially been reduced as it was for equivalent first trimester samples, but that the testosterone production recovered during the xenografting period.

Separating Effects of Nodal and Activin Signaling in First Trimester Testis Cultures

The effects of SB431542 described above could be due to the inhibition of Nodal, Activin, and/or growth differentiation factor (GDF) signaling, although based on previous studies in fetal mice testes, the effects are most likely mediated via Nodal or Activin pathways (Spiller et al., 2012; Souquet et al., 2012; Wu et al., 2013; Miles et al., 2013). To determine the relative contribution of Nodal and Activin signaling, experiments were conducted to inhibit or stimulate the two pathways separately (Figure 4A). Activin signaling was stimulated by treatment with recombinant Activin A and inhibited with follistatin, while Nodal signaling was stimulated by treatment with recombinant Nodal and inhibited by Lefty.

Inhibition of Nodal signaling by Lefty treatment in first trimester fetal testis *ex vivo* cultures resulted in effects resembling those observed after simultaneous inhibition of Nodal and Activin (Figure 4B). Treatment with Lefty appeared to reduce the number of $OCT4^+$ gonocytes, disrupted seminiferous cord structures, and reduced AMH expression (Figure 4B). The effects of Nodal inhibition alone were less severe compared to SB431542-treated samples, but the inhibition of Nodal signaling was likely the main driver of the severe morphological changes and disruption of seminiferous cord formation that were observed after simultaneous inhibition of Nodal and Activin signaling with SB431542 (Figure 4B). In accordance, inhibition of the Activin pathway in cultures of first trimester fetal testis did not result in any major testicular effects on morphology or the expression pattern of germ cell, Sertoli cell, or interstitial cell markers (Figure S5).

The quantification of gonocytes in Lefty-treated fetal testis samples confirmed that a significantly ($p < 0.05$) lower number of $OCT4^+$ cells per square millimeter were present (Figure 5A), suggesting a role for Nodal signaling in germ cell survival. Stimulation of Nodal signaling in *ex vivo* cultures of first trimester fetal testes resulted in a significant ($p < 0.05$) increase in the number of $OCT4^+$ gonocytes compared to vehicle controls (Figure 5A), as well as a significant ($p < 0.05$) increase in AMH secretion compared to vehicle controls (Figure 5B). No effects on gross

interstitial cells), and CYP11A1 (fetal Leydig cell marker). Counterstaining with Mayer's hematoxylin; scale bar corresponds to 50 μm. Bottom: triple immunofluorescence with OCT4 (red), MAGE-A4 (green), and SOX9 (Sertoli cell marker, blue). Tissue from three fetuses was investigated.

(C) Quantification of germ cells per square millimeter was determined as the number of $OCT4^+$ and $MAGE\text{-}A4^+$ cells. Values represent means ± SEMs, with n = 3. Significant difference compared to vehicle controls, $^*p < 0.05$.

(D) Testosterone production by the first trimester fetal testis tissue grafted into castrated nude mice. Seminal vesicle weight calculated as a ratio compared to vehicle controls and testosterone levels (ng/mL) in mouse serum determined by radioimmunoassay (RIA). Values represent means ± SEMs, with n = 3. Significant difference compared to vehicle controls, $^*p < 0.05$.

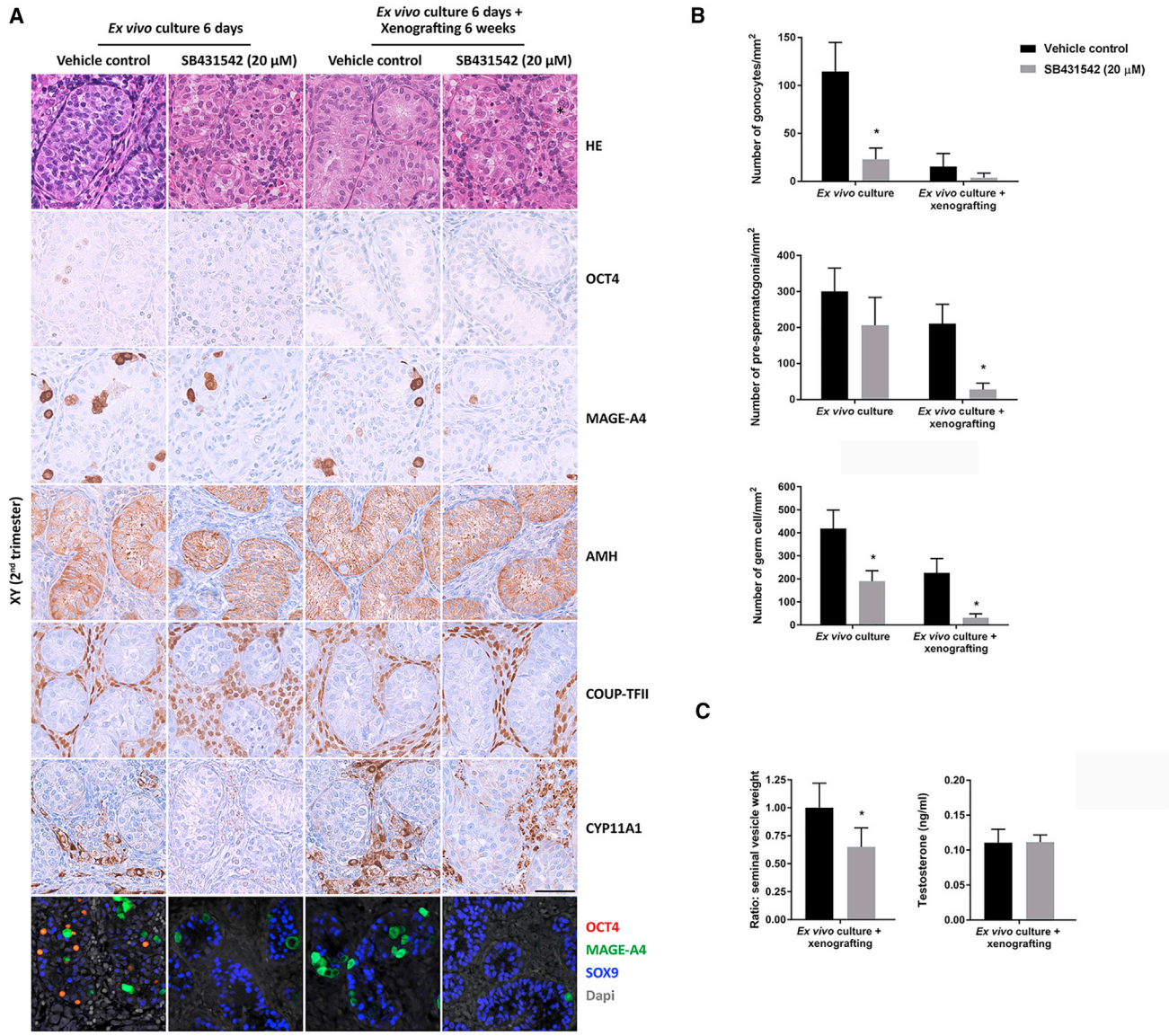

Figure 3. Long-Term Effects of Simultaneous Inhibition of Nodal and Activin Signaling in Second Trimester Human Fetal Testes

A) Effects of initial short-term (6 days) treatment with SB431542 (20 μM), followed by xenografting for 6 weeks (without treatment) on tissue morphology and expression of germ cell and somatic cell markers in second trimester fetal testis samples. Cultured and grafted samples (±SB431542) are compared to samples from the same fetus, which has been cultured only *ex vivo* (±SB431542). Immunohistochemical staining include OCT4 and MAGE-A4 (germ cell markers), AMH (Sertoli cell marker), COUP-TFII (marker of interstitial cells), and CYP11A1 (fetal Leydig cell marker). Counterstaining with Mayer's hematoxylin; scale bar corresponds to 50 μm. *Multinucleated germ cell; see also higher-magnification image in Figure S4. Bottom: triple immunofluorescence with OCT4 (red), MAGE-A4 (green), and SOX9 (Sertoli cell marker, blue). Tissue from five fetuses was investigated.

(B) Quantification of germ cells was determined as the number of gonocytes ($OCT4^+$) per square millimeter, pre-spermatogonia ($MAGE\text{-}A4^+$) per square millimeter, and total number of germ cells ($OCT4^+$ + $MAGE\text{-}A4^+$) per square millimeter. Values represent means ± SEMs, with n = 5. Significant difference compared to vehicle controls, *$p < 0.05$.

(C) Testosterone production by the second trimester fetal testis tissue grafted into castrated nude mice. Seminal vesicle weight calculated as a ratio compared to vehicle controls and testosterone levels (ng/mL) in mouse serum determined by RIA. Values represent means ± SEMs, with n = 5. Significant difference compared to vehicle controls, *$p < 0.05$.

morphology and overall expression of Sertoli cell or interstitial cell markers, cell proliferation, or apoptosis were found after Nodal treatment (Figures 4B and S6). In contrast, stimulation of Activin signaling in fetal testis cultures did not affect the number of $OCT4^+$ gonocytes or AMH secretion (Figures 5C and 5D). Inhibition of the Activin pathway following follistatin treatment resulted in a significantly ($p < 0.05$) lower number of $OCT4^+$ cells per square millimeter (Figure 5C), while no effect on AMH secretion was found (Figure 5D). These findings suggest an overlapping function of Nodal and Activin pathways in mediating germ

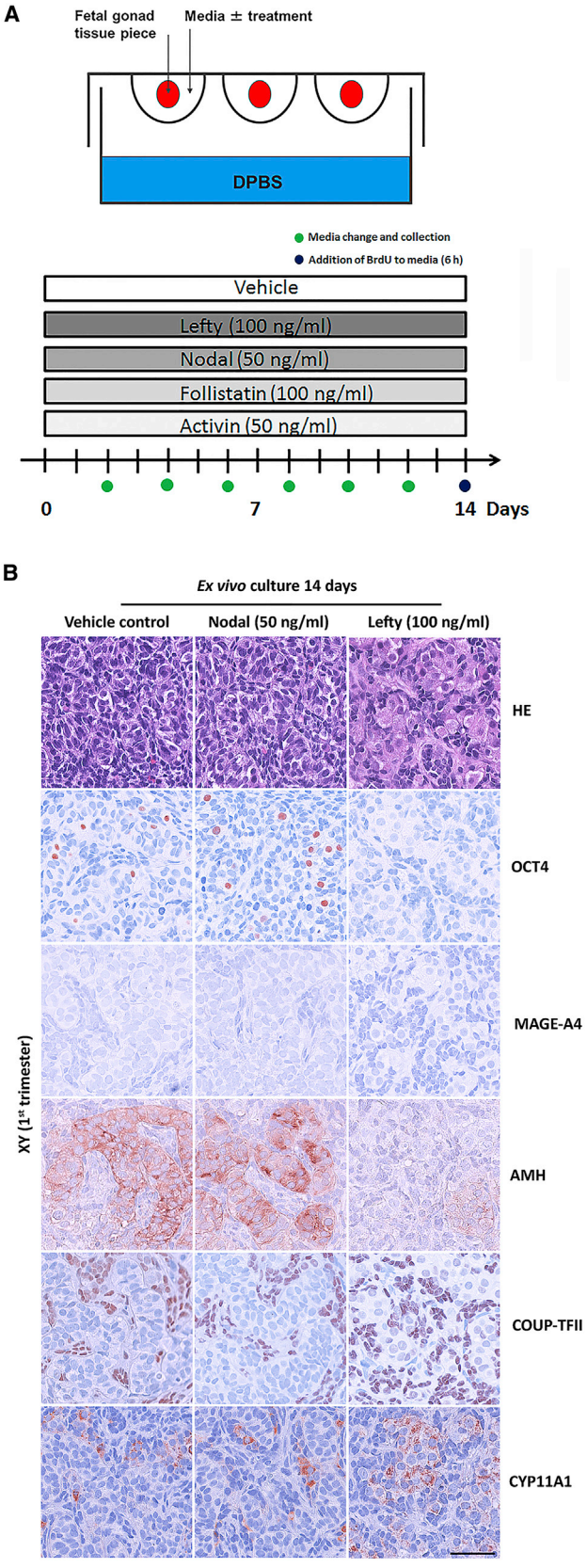

Figure 4. Effects of Manipulating Nodal Signaling in First Trimester Fetal Testis *Ex Vivo* Cultures

(A) Experimental overview of treatment with recombinant Nodal (50 ng/mL), Lefty (100 ng/mL), Activin A (50 ng/mL), and follistatin (100 ng/mL) for 14 days in *ex vivo* culture of human fetal testes.

(B) Morphology and expression pattern of germ cell markers OCT4 (gonocytes) and MAGE-A4 (pre-spermatogonia), Sertoli cell marker (AMH), interstitial cell marker (COUP-TFII), and fetal Leydig cell marker (CYP11A1) investigated in first trimester fetal testis samples treated with Nodal and Lefty. n = 7 fetuses for Nodal treatment and n = 12 for Lefty treatment. Counterstaining with Mayer's hematoxylin; scale bar corresponds to 50 μm.

cell survival in fetal testis. Stimulation of the Nodal pathway also affected androgen production, with significantly ($p < 0.05$) higher levels of androstenedione and dehydroepiandrosterone sulfate (DHEAS) and significantly ($p < 0.05$) lower levels of 17-hydroxy-progesterone (17-OHP) and cortisone compared to vehicle-treated controls (Figure 5E). In contrast, Lefty treatment did not affect steroidogenesis (Figure 5E), which is in accordance with the observed Leydig cell expression of CYP11A1 that appeared unaltered compared to the vehicle control (Figure 4B).

Manipulation of the Nodal pathway did not appear to affect the expression of proliferation (BrdU) and apoptosis (cPARP) markers (Figure S6A), and this observation was confirmed after the quantification of $BrdU^+$ germ cells and $cPARP^+$ cells per square millimeter, demonstrating no difference between Nodal and Lefty treatment compared to vehicle controls (Figure S6B). Although a tendency toward a lower number of proliferating germ cells and an increased number of apoptotic cells was found in Lefty-treated testis samples (Figure 6B), which is in line with the finding of a reduced number of gonocytes ($OCT4^+$) in fetal testes following Lefty treatment (Figure 5A). No effects on apoptosis and proliferation of germ cells were observed after manipulation of the Activin pathway (Figure S7A), despite a tendency toward a lower number of proliferating germ cells and a higher number of apoptotic cells after follistatin treatment (Figure S7B). Also, no effects on steroidogenesis were detected after Activin and follistatin treatment in fetal testis (Figure S7C). These results suggest that Nodal signaling is involved in the regulation of pluripotency factor expression in germ cells, in establishment of seminiferous cords, and may also play a role in steroidogenesis by stimulating androgen production in fetal Leydig cells.

Stimulation of Nodal Signaling in Second Trimester Fetal Testes

To investigate the long-term consequences of stimulating Nodal signaling, second trimester fetal testis samples containing a mixture of gonocytes ($OCT4^+$) and pre-spermatogonia ($MAGE\text{-}A4^+$) were treated with recombinant Nodal for 10 days in *ex vivo* culture, followed by xenografting for 6 weeks (Figure 6A). Again, no apparent effects on morphology, overall expression of Sertoli cells, or interstitial cell markers were found (Figure 6B), and there was no difference in serum testosterone or seminal vesicle weight between host mice grafted with Nodal-treated samples and mice grafted with vehicle-treated samples (Figure 6C). Interestingly, $OCT4^+$ gonocytes were present in the Nodal-treated samples after xenografting, whereas very few $OCT4^+$ germ cells were observed in vehicle-treated control samples, in which the majority of germ cells present

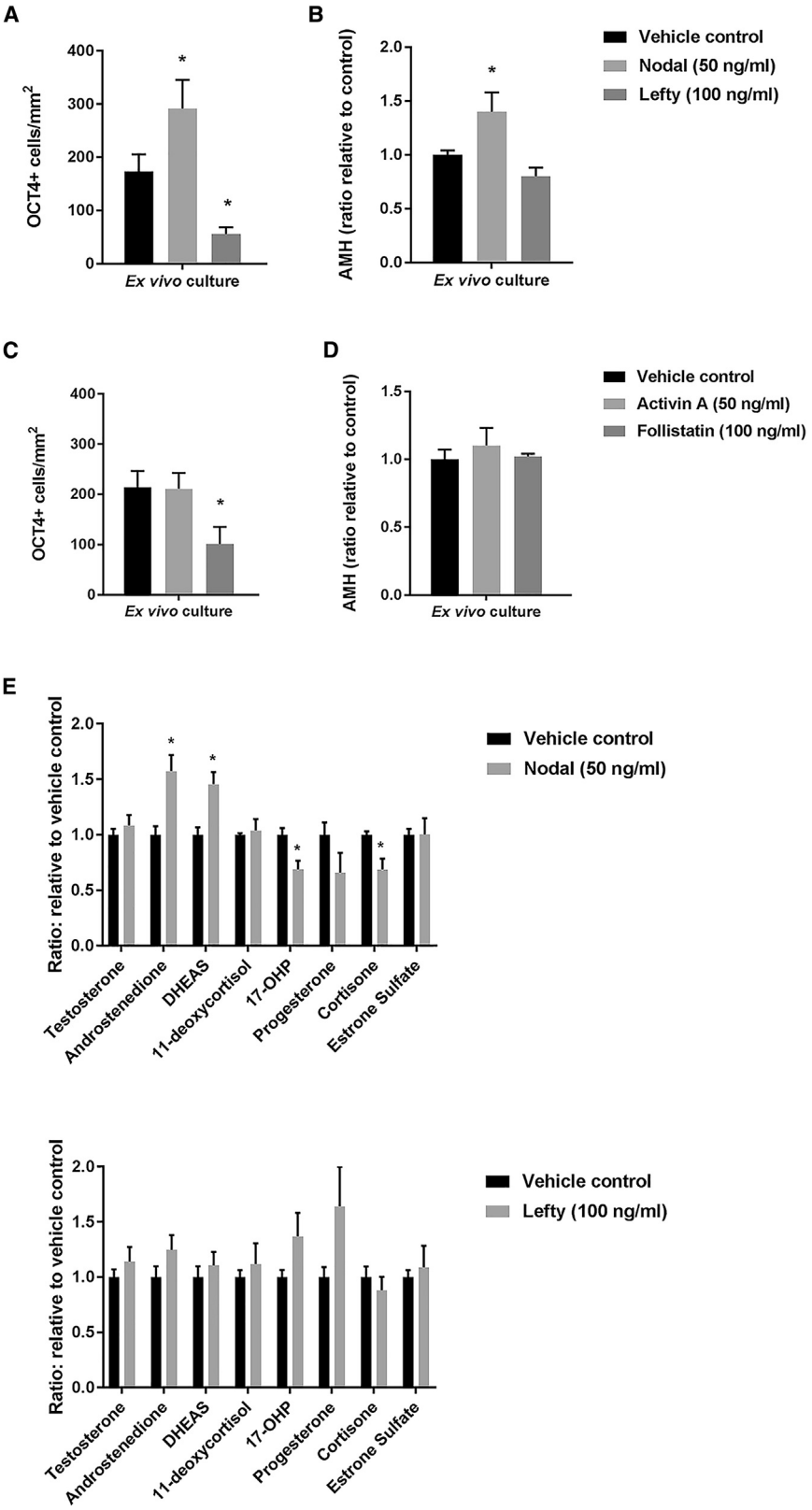

Figure 5. Effects of Manipulating Nodal and Activin Signaling Seperately in First Trimester Fetal Testis *Ex Vivo* Cultures

(A) Quantification of gonocytes determined as the number of $OCT4^+$ cells per square millimeter in samples treated with recombinant Nodal (50 ng/mL) and Lefty (100 ng/mL) for 14 days in *ex vivo* culture. Values represent means ± SEMs, with n = 7 (Nodal) and n = 12 (Lefty). *Significant difference compared to vehicle controls, *$p < 0.05$.

(B) Quantification of AMH produced by the fetal testis tissue in *ex vivo* cultures exposed to Nodal and Lefty and secreted into the media. Medium was collected every 48 hr throughout the 14-day culture period and pooled for each individual tissue piece. AMH was measured by ELISA and is shown as a ratio compared to vehicle controls. Values represent means ± SEMs, with n = 7 (Nodal) and n = 12 (Lefty). *Significant difference ($p < 0.05$) compared to vehicle controls.

(C) Quantification of gonocytes determined as the number of $OCT4^+$ cells per square millimeter in samples treated with recombinant Activin A (50 ng/mL) and follistatin (100 ng/mL) for 14 days in *ex vivo* culture. Values represent means ± SEMs, with n = 9 (Activin A) and n = 7 (follistatin). Significant difference compared to vehicle controls, *$p < 0.05$.

(D) Quantification of AMH produced by the fetal testis tissue in *ex vivo* cultures exposed to Activin and follistatin and secreted into the media. AMH was measured by ELISA and is shown as a ratio compared to vehicle controls. Values represent means ± SEMs, with n = 9 (Activin A) and n = 7 (follistatin).

(E) Quantification of androgens produced in the fetal testis tissue *ex vivo* cultures and secreted into the media droplets. Medium was collected every 48 hr throughout the 14 weeks of culture and pooled for each individual tissue piece. Androgens were measured by LC-MS/MS and are shown as ratios compared to the corresponding vehicle controls for each metabolite. Values represent means ± SEMs, with n = 7 (Nodal) and n = 12 (Lefty). Significant difference compared to vehicle controls, *$p < 0.05$.

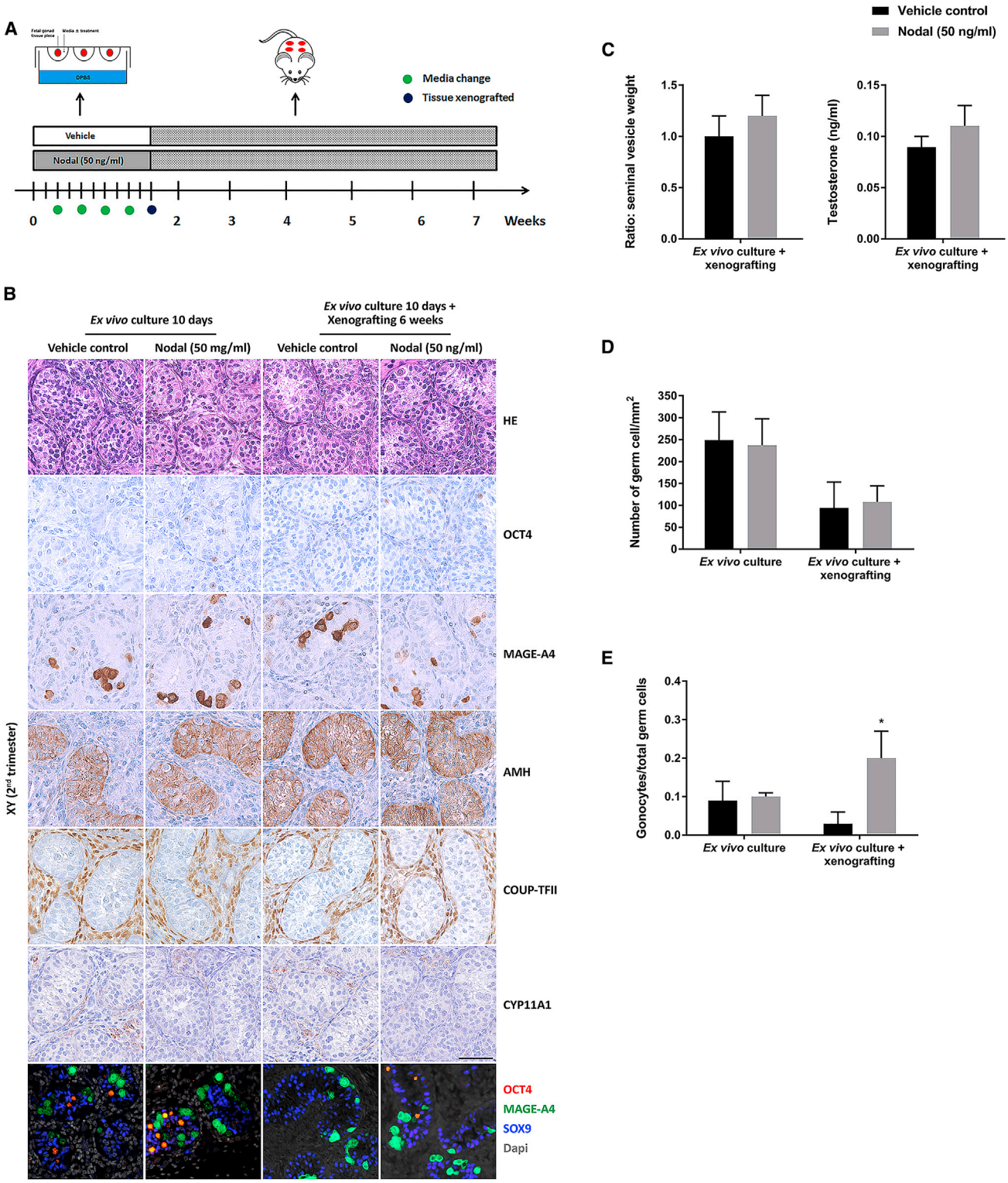

Figure 6. Long-Term Effects of Stimulating the Nodal Signaling Pathway in Second Trimester Human Fetal Testes

(A) Experimental overview of treatment with Nodal for 10 days in *ex vivo* culture, followed by xenografting for 6 weeks (without treatment).

(B) Effects of initial short-term treatment with Nodal (50 ng/mL), followed by xenografting on tissue morphology and expression of germ cell and somatic cell markers in second trimester fetal testis samples. Cultured and grafted samples (±Nodal) are compared to samples from the same fetus, which has been cultured only *ex vivo* (±Nodal). Immunohistochemical staining include OCT4 and MAGE-A4 (germ cell markers), AMH (Sertoli cell marker), COUP-TFII (marker of interstitial

(legend continued on next page)

were MAGE-A4$^+$ pre-spermatogonia (Figure 6B). Stimulation of the Nodal pathway in second trimester fetal testis samples appeared to prevent germ cell differentiation because the total number of germ cells per area was unaffected when examined both after *ex vivo* culture alone or after *ex vivo* culture and subsequent xenografting (Figure 6D). Consequently, the ratio of gonocytes to the total number of germ cells was significantly increased ($p < 0.05$) in Nodal-stimulated fetal testis tissue after the xenografting period (Figure 6E). This finding most likely reflects a prolonged maintenance of OCT4$^+$ expression in gonocytes in fetal testes following the initial stimulation of Nodal signaling.

DISCUSSION

Despite growing evidence that human fetal testis development and dysfunction may be a critical determinant of the later risk of several reproductive disorders included in the testicular dysgenesis syndrome, the underlying molecular mechanisms and signaling pathways are largely unknown. The present study contributed to elucidating this deficiency by combining *ex vivo* tissue culture and xenograft approaches, thereby demonstrating that Nodal and Activin signaling control distinct processes during human testicular development and male germ cell differentiation, but with some overlap in function between the two pathways. Our study shows that the Nodal signaling pathway is involved in regulating the expression of pluripotency factors in human fetal germ cells and plays a role in the establishment of seminiferous cords.

We found that simultaneous inhibition of Nodal and Activin signaling by SB431542 exposure in the cultures of first trimester fetal testes caused a complete loss of the gonocyte population and disruption of seminiferous cord formation, reduced the expression of somatic lineage markers, reduced the secretion of AMH, and impaired steroidogenesis. Some of these effects are in accordance with previous results from mouse studies, including disruption of seminiferous cords and distorted arrangement of somatic cells, which were found in fetal mouse testes treated with SB431542 (Wu et al., 2013; Miles et al., 2013). We found reduced androgen production and accumulation of steroidogenic precursors, consistent with impaired CYP17A1 activity, but effects on steroidogenesis have not previously been reported after simultaneous inhibition of Nodal and Activin signaling. The SB431542-induced loss of gonocytes in the human fetal testis was more severe compared to the germ cell effects reported in mice in which only a minor reduction in germ cell survival and premature initiation of meiosis was found (Souquet et al., 2012; Wu et al., 2013). Our finding of both reduced germ cell proliferation and increased apoptosis in fetal testes treated with SB431542 does not exclude the possibility of simultaneous accelerated differentiation of the remaining germ cell population, as was previously reported in a mouse model with compromised Nodal signaling (Spiller et al., 2012). However, because we found no parallel increase in the number of pre-spermatogonia (MAGE-A4$^+$ and/or VASA$^+$) or meiotic (SCP3$^+$) germ cells after SB431542 exposure, even after xenografting, it is most likely that the gonocytes had been lost. This species difference in the effects on germ cells following manipulation of Nodal signaling could be attributed to different experimental approaches or differences in the regulation of pluripotency factors, with gradual asynchronous transition from gonocyte to pre-spermatogonia in humans and a more synchronized germ cell differentiation process in rodents (Mitchell et al., 2008). Further evidence of dissimilarity in the role of Nodal signaling between humans and mice is the observation that Nodal pathway genes are expressed in fetal germ cells in both testes and ovaries in humans (Li et al., 2017), while expression is predominantly found in male germ cells in fetal mouse gonads (Souquet et al., 2012; Spiller et al., 2012; Wu et al., 2013; Miles et al., 2013).

The majority of the effects observed in first trimester fetal testes after SB431542-induced simultaneous Nodal and Activin inhibition were rescued with time after xenografting, including the re-establishment of seminiferous cords and a normal expression pattern of somatic cell markers. The exceptions were the observed effects on androgen production, which was still reduced after the xenografting period, and the loss of the gonocyte population. The latter was not rescued after xenografting, which is consistent with an initial SB431542-induced loss of these cells by reduced proliferation and increased apoptosis rather than there being, for example, downregulation of pluripotency factors without the simultaneous upregulation of more differentiated germ cell markers. In comparison, the effects of the simultaneous inhibition of Nodal and Activin signaling in second trimester fetal testis samples were less severe than in first trimester samples, with a reduced number and an altered morphology of germ cells and a reduced seminal vesicle weight in mice grafted with SB431542-treated tissue being the main effects. The androgen production was less affected by the end of the xenografting period, with no difference in serum testosterone between mice grafted with fetal testis tissue initially treated with SB431542, and vehicle control. The finding of a subpopulation of multinucleated pre-spermatogonia is interesting because this abnormality has been observed in cryptorchid boys, some of whom also had GCNIS (Cortes et al., 2003). Also, multinucleated germ cells are a feature of testicular dysgenesis syndrome in fetal rats following *in utero* exposure to the plasticizer di-*n*-butyl-phthalate (DBP) and are also observed in human fetal testis xenografts following DBP exposure (Heger et al., 2012; van den Driesche et al., 2015a). This

cells), and CYP11A1 (fetal Leydig cell marker). Counterstaining with Mayer's hematoxylin; scale bar corresponds to 50 μm. Bottom: triple immunofluorescence with OCT4 (red), MAGE-A4 (green), and SOX9 (Sertoli cell marker, blue). Tissue from three fetuses was investigated.

(C) Testosterone production by the fetal second trimester fetal testis tissue grafted into castrated nude mice. Seminal vesicle weight calculated as a ratio compared to vehicle controls and testosterone levels (ng/mL) in mouse serum determined by RIA. Values represent means ± SEMs, with n = 3.

(D) Quantification of germ cells per square millimeter was determined as the number of OCT4$^+$ and MAGE-A4$^+$ cells. Values represent means ± SEMs, with n = 3.

(E) Ratio of gonocytes/total germ cells corresponds to the number of OCT4$^+$ cells/(OCT4$^+$ + MAGE-A4$^+$ cells). Values represent means ± SEMs, with n = 3. Significant difference compared to vehicle controls, *$p < 0.05$.

supports the concept that the disruption of Nodal and Activin signaling in the human fetal testis contributes to a testicular dysgenesis syndrome phenotype. However, the complete testicular dysgenesis that is observed after experimental inhibition of Nodal and Activin signaling in first trimester fetal testes constitute a more severe phenotype than the focal disruption that is most often observed in testicular tissue from adult patients with testicular dysgenesis syndrome (Hoei-Hansen et al., 2003; Rajpert-De Meyts et al., 2013), making direct comparison of the consequent effects on germ cells difficult.

Separating the roles of Nodal signaling and Activin signaling in first trimester human fetal testes development by individually stimulating and inhibiting each signaling pathway clearly demonstrated that these two pathways have distinct but partly overlapping roles during human fetal testis development. The opposing effects of Nodal and Lefty treatment on the number of OCT4$^+$ gonocytes indicate that the Nodal pathway is a direct regulator of the expression of pluripotency factors in the human fetal testis. Because the expression of *Cripto* is triggered by fibroblast growth factor 9 (FGF9) in fetal mouse testes, resulting in the initiation of signaling through the Nodal pathway (Spiller et al., 2012), it would be relevant to examine the involvement of the FGF9 pathway in human fetal testis development in future studies. The other distinct finding of our study implicating Nodal signaling in the establishment of seminiferous cords is most likely an indirect effect. In mice, disruption of seminiferous cords was also evident following the simultaneous inhibition of Nodal and Activin signaling (Wu et al., 2013; Miles et al., 2013). The formation and organization of seminiferous cords in mice is known to depend on endothelial cell migration from the mesonephros, with disrupted cord formation observed after inhibition of the migration of these cells, but without effects on Sertoli cell expression of SOX9 (Combes et al., 2009). These findings closely resemble the phenotype observed in human testes in the present study and suggest that the Nodal pathway could also be involved in regulating endothelial cell migration in early testicular organogenesis in humans, although this remains to be elucidated. The reduced number of OCT4$^+$ gonocytes resulting from the inhibition of Nodal signaling may also involve indirect effects in addition to the direct regulation of pluripotency factor expression, because the disrupted seminiferous cords result in impaired germ cell-somatic niche interaction, which is likely to also affect gonocyte survival and proliferation. Because there was also a reduced number of gonocytes in follistatin-treated samples, it indicates that both Nodal and Activin are involved in germ cell survival and proliferation. This is in accordance with a previous study showing that Activin A stimulates human oogonial survival (Martins da Silva et al., 2004) and the notion that also TGF-β and GDF mediates signals through ALK4/5/7, which could contribute to the more severe effects of SB431542 compared to Lefty and follistatin treatments. Moreover, the complete loss of gonocytes observed in second trimester fetal testes following the simultaneous inhibition of Nodal and Activin indicates that the effect of Nodal inhibition is a direct effect because the seminiferous cords were not disrupted in these samples. Specific inhibition of the Nodal pathway by Lefty treatment in first trimester fetal testes resulted in effects on the somatic cells and seminiferous cords that resembled the effects of simultaneous inhibition of Nodal and Activin, with seminiferous cords almost completely disrupted and a clear reduction in Sertoli cell AMH immunoexpression, although the secretion of AMH to the media of *ex vivo* cultures was not affected. Also, inhibition of Nodal and Activin pathways separately did not appear to affect the fetal Leydig cells, since no effects on steroidogenesis or expression of CYP11A1 were observed, perhaps indicating some redundancy between these signaling pathways in the regulation of fetal Leydig cell function.

Stimulation of Nodal signaling in first trimester fetal testes distinctly increased the number of OCT4$^+$ gonocytes, and a similar effect was found in second trimester fetal testes in which the expression of pluripotency factors is normally downregulated as part of the transition from gonocyte to pre-spermatogonium. The effects of short-term stimulation of the Nodal pathway in culture persisted for up to 6 weeks after xenografting, indicating that the physiological regulation of gonocyte to pre-spermatogonia transition in human fetal testes may involve Nodal signaling. This finding has implications for our understanding of the first step in the development of testicular GCNIS, which are considered to be arrested fetal gonocytes persisting within the testis (Rajpert-De Meyts et al., 2016; Skakkebaek et al., 1987). The current model for the pathogenesis of testicular germ cell cancer proposes that the arrest of fetal gonocyte differentiation is the result of altered signaling from the surrounding somatic cells, including in particular reduced androgen stimulation and testicular dysgenesis (Skakkebaek et al., 2001; Rajpert-De Meyts and Skakkebaek, 1993). In this study, we have demonstrated reduced androgen production and complete disruption of seminiferous cords in the first trimester fetal human testis following SB431542-induced simultaneous inhibition of Nodal and Activin signaling, but without any indication of an increased number of gonocytes. The SB431542-induced widespread dysgenesis and pronounced reduction in androgen production did not lead to the arrest of gonocyte differentiation; rather, this cell population was lost. Conversely, the stimulation of Nodal signaling in first trimester fetal testis samples that resulted in an increased number of gonocytes also caused an increase in the production of androgen precursors. This is in contrast to the proposed mechanism of reduced masculinization resulting in prolonged expression of pluripotency factors in human fetal gonocytes in the pathogenesis of testicular germ cell cancer. Despite this, the finding of prolonged expression of OCT4 in human fetal gonocytes after the stimulation of Nodal signaling provides insight into a possible mechanism for the development of the testicular cancer precursor GCNIS, which, based on the findings in this study, could involve focal dysregulation of the Nodal pathway. However, independent validation and further studies are needed to corroborate this hypothesis.

In conclusion, the present study demonstrated a key role of Nodal signaling in regulating the expression of pluripotency factors in human fetal germ cells and in the establishment of seminiferous cords during early human fetal testis development. Moreover, we found that the Nodal and Activin signaling pathways cooperate in mediating fetal germ cell survival and proliferation as well as AMH secretion by immature Sertoli cells and steroidogenesis by the fetal Leydig cells. The effects on seminiferous cord structure and expression of somatic cell

markers following the simultaneous inhibition of Nodal signaling and Activin signaling were reversible, while the effects on germ cells and steroidogenesis were not. The present study substantially adds to the understanding of early events in human fetal testis development. Our findings delineate the consequences of dysregulating Nodal and Activin signaling in the human fetal testis, which have important implications for understanding male reproductive disorders, including in particular testicular dysgenesis syndrome and the pathogenesis of germ cell neoplasia.

STAR★METHODS

Detailed methods are provided in the online version of this paper and include the following:

- KEY RESOURCES TABLE
- CONTACT FOR REAGENT AND RESOURCE SHARING
- EXPERIMENTAL MODEL AND SUBJECT DETAILS
  - Collection of human fetal gonads in Denmark
  - Collection of human fetal gonads in UK
  - Nude mice
- METHOD DETAILS
  - *Ex vivo* testis tissue culture
  - Grafting of human fetal testis tissue into nude mice
  - Immunohistochemistry
  - Immunofluorescence
  - BrdU incorporation
  - Quantification of germ cells
  - TUNEL assay
  - Quantification of testosterone in mice
  - Steroid hormone measurements in culture medium
  - AMH measurements in culture medium
  - Quantitative RT-PCR
- QUANTIFICATION AND STATISTICAL ANALYSIS

SUPPLEMENTAL INFORMATION

Supplemental Information includes seven figures and three tables and can be found with this article online at https://doi.org/10.1016/j.celrep.2018.10.064.

ACKNOWLEDGMENTS

The authors wish to thank the staff members at the Departments of Gynaecology at Rigshospitalet and Hvidovre Hospital for their help with the collection of the fetal tissue. The excellent technical assistance of the technicians at the Department of Growth and Reproduction, especially Ana Ricci Nielsen, Camilla Tang Thomsen, and Brian Vendelbo Hansen, is gratefully acknowledged. We gratefully appreciate the work of Anne Saunderson and the staff of the Bruntsfield Suite of the Royal Infirmary of Edinburgh for their provision of fetal tissue, as well as the Human Developmental Biology Resource (www.hdbr.org) for providing some of the fetal material (Joint MRC/Wellcome Trust grant no. 099175/Z/12/Z). We would also like to acknowledge William Mungall for assistance with the animal work. We appreciate the kind gift of the FOXL2 antibody from Dr. D. Wilhelm (University of Melbourne) and the MAGE-A4 antibody from Prof. G. Spagnoli (University of Basel). This work was supported in part by a European Society for Paediatric Endocrinology (ESPE) Research Fellowship, sponsored by Novo Nordisk A/S, to A. Jørgensen. Additional funding for this project was obtained from the Danish Cancer Society (grant no. R72-A4335-13-S2, to A. Jørgensen), the Research Council of the Capital Region of Denmark (to E.R.D.M.), a Wellcome Trust Intermediate Clinical Fellowship (grant no. 098522, to R.T.M.), The MRC Centre for Reproductive Health is supported by an MRC Centre Grant (MR/N022556/1). The Research Fund at Rigshospitalet (to A. Juul and J.E.N.), The Erichssen Family Fund (to A. Jørgensen), Dagmar Marshalls Fund (to A. Jørgensen), and the Aase & Ejnar Danielsens Fund (to A. Jørgensen).

AUTHOR CONTRIBUTIONS

A. Jørgensen, E.R.D.M., and R.T.M. conceived the project. A. Jørgensen, J.M., J.E.N., K.R.K., and H.F. performed the experiments. L.L., S.P., L.L.T., and K.J.H. provided the tissue. A. Jørgensen, A.-M.A., N.E.S., A. Juul, R.M.S., E.R.D.M., and R.T.M. analyzed and discussed the data. A. Jørgensen, A. Juul, R.M.S., E.R.d.M., and R.T.M. wrote the manuscript. All of the authors approved the submitted manuscript.

DECLARATION OF INTERESTS

The authors declare no competing interests.

Received: May 21, 2018
Revised: September 14, 2018
Accepted: October 17, 2018
Published: November 13, 2018

REFERENCES

Bendsen, E., Byskov, A.G., Laursen, S.B., Larsen, H.P., Andersen, C.Y., and Westergaard, L.G. (2003). Number of germ cells and somatic cells in human fetal testes during the first weeks after sex differentiation. Hum. Reprod. *18*, 13–18.

Berta, P., Hawkins, J.R., Sinclair, A.H., Taylor, A., Griffiths, B.L., Goodfellow, P.N., and Fellous, M. (1990). Genetic evidence equating SRY and the testis-determining factor. Nature *348*, 448–450.

Combes, A.N., Wilhelm, D., Davidson, T., Dejana, E., Harley, V., Sinclair, A., and Koopman, P. (2009). Endothelial cell migration directs testis cord formation. Dev. Biol. *326*, 112–120.

Corker, C.S., and Davidson, D.W. (1978). A radioimmunoassay for testosterone in various biological fluids without chromatography. J. Steroid Biochem. *9*, 373–374.

Cortes, D., Thorup, J., and Visfeldt, J. (2003). Multinucleated spermatogonia in cryptorchid boys: a possible association with an increased risk of testicular malignancy later in life? APMIS *111*, 25–31.

Evtouchenko, L., Studer, L., Spenger, C., Dreher, E., and Seiler, R.W. (1996). A mathematical model for the estimation of human embryonic and fetal age. Cell Transplant. *5*, 453–464.

Gaskell, T.L., Esnal, A., Robinson, L.L., Anderson, R.A., and Saunders, P.T. (2004). Immunohistochemical profiling of germ cells within the human fetal testis: identification of three subpopulations. Biol. Reprod. *71*, 2012–2021.

Hanley, N.A., Hagan, D.M., Clement-Jones, M., Ball, S.G., Strachan, T., Salas-Cortés, L., McElreavey, K., Lindsay, S., Robson, S., Bullen, P., et al. (2000). SRY, SOX9, and DAX1 expression patterns during human sex determination and gonadal development. Mech. Dev. *91*, 403–407.

Heger, N.E., Hall, S.J., Sandrof, M.A., McDonnell, E.V., Hensley, J.B., McDowell, E.N., Martin, K.A., Gaido, K.W., Johnson, K.J., and Boekelheide, K. (2012). Human fetal testis xenografts are resistant to phthalate-induced endocrine disruption. Environ. Health Perspect. *120*, 1137–1143.

Hoei-Hansen, C.E., Holm, M., Rajpert-De Meyts, E., and Skakkebaek, N.E. (2003). Histological evidence of testicular dysgenesis in contralateral biopsies from 218 patients with testicular germ cell cancer. J. Pathol. *200*, 370–374.

Hoei-Hansen, C.E., Nielsen, J.E., Almstrup, K., Sonne, S.B., Graem, N., Skakkebaek, N.E., Leffers, H., and Rajpert-De Meyts, E. (2004). Transcription factor AP-2gamma is a developmentally regulated marker of testicular carcinoma in situ and germ cell tumors. Clin. Cancer Res. *10*, 8521–8530.

Honecker, F., Stoop, H., de Krijger, R.R., Chris Lau, Y.F., Bokemeyer, C., and Looijenga, L.H. (2004). Pathobiological implications of the expression of markers of testicular carcinoma in situ by fetal germ cells. J. Pathol. *203*, 849–857.

James, D., Levine, A.J., Besser, D., and Hemmati-Brivanlou, A. (2005). TGFbeta/activin/nodal signaling is necessary for the maintenance of pluripotency in human embryonic stem cells. Development *132*, 1273–1282.

Jørgensen, A., and Rajpert-De Meyts, E. (2014). Regulation of meiotic entry and gonadal sex differentiation in the human: normal and disrupted signaling. Biomol. Concepts *5*, 331–341.

Jørgensen, N., Rajpert-De Meyts, E., Graem, N., Müller, J., Giwercman, A., and Skakkebaek, N.E. (1995). Expression of immunohistochemical markers for testicular carcinoma in situ by normal human fetal germ cells. Lab. Invest. *72*, 223–231.

Jørgensen, A., Nielsen, J.E., Blomberg Jensen, M., Græm, N., and Rajpert-De Meyts, E. (2012). Analysis of meiosis regulators in human gonads: a sexually dimorphic spatio-temporal expression pattern suggests involvement of DMRT1 in meiotic entry. Mol. Hum. Reprod. *18*, 523–534.

Jørgensen, A., Nielsen, J.E., Almstrup, K., Toft, B.G., Petersen, B.L., and Rajpert-De Meyts, E. (2013). Dysregulation of the mitosis-meiosis switch in testicular carcinoma in situ. J. Pathol. *229*, 588–598.

Jørgensen, A., Young, J., Nielsen, J.E., Joensen, U.N., Toft, B.G., Rajpert-De Meyts, E., and Loveland, K.L. (2014). Hanging drop cultures of human testis and testis cancer samples: a model used to investigate activin treatment effects in a preserved niche. Br. J. Cancer *110*, 2604–2614.

Jørgensen, A., Nielsen, J.E., Perlman, S., Lundvall, L., Mitchell, R.T., Juul, A., and Rajpert-De Meyts, E. (2015). Ex vivo culture of human fetal gonads: manipulation of meiosis signalling by retinoic acid treatment disrupts testis development. Hum. Reprod. *30*, 2351–2363.

Li, L., Dong, J., Yan, L., Yong, J., Liu, X., Hu, Y., Fan, X., Wu, X., Guo, H., Wang, X., et al. (2017). Single-Cell RNA-Seq Analysis Maps Development of Human Germline Cells and Gonadal Niche Interactions. Cell Stem Cell *20*, 858–873.e4.

Martins da Silva, S.J., Bayne, R.A., Cambray, N., Hartley, P.S., McNeilly, A.S., and Anderson, R.A. (2004). Expression of activin subunits and receptors in the developing human ovary: activin A promotes germ cell survival and proliferation before primordial follicle formation. Dev. Biol. *266*, 334–345.

Miles, D.C., Wakeling, S.I., Stringer, J.M., van den Bergen, J.A., Wilhelm, D., Sinclair, A.H., and Western, P.S. (2013). Signaling through the TGF beta-activin receptors ALK4/5/7 regulates testis formation and male germ cell development. PLoS One *8*, e54606.

Mitchell, R.T., Cowan, G., Morris, K.D., Anderson, R.A., Fraser, H.M., Mckenzie, K.J., Wallace, W.H., Kelnar, C.J., Saunders, P.T., and Sharpe, R.M. (2008). Germ cell differentiation in the marmoset (Callithrix jacchus) during fetal and neonatal life closely parallels that in the human. Hum. Reprod. *23*, 2755–2765.

Mitchell, R.T., Saunders, P.T., Childs, A.J., Cassidy-Kojima, C., Anderson, R.A., Wallace, W.H., Kelnar, C.J., and Sharpe, R.M. (2010). Xenografting of human fetal testis tissue: a new approach to study fetal testis development and germ cell differentiation. Hum. Reprod. *25*, 2405–2414.

Ostrer, H., Huang, H.Y., Masch, R.J., and Shapiro, E. (2007). A cellular study of human testis development. Sex Dev. *1*, 286–292.

Papanayotou, C., and Collignon, J. (2014). Activin/Nodal signalling before implantation: setting the stage for embryo patterning. Philos. Trans. R. Soc. Lond. B Biol. Sci. *369*, 1657.

Pauls, K., Schorle, H., Jeske, W., Brehm, R., Steger, K., Wernert, N., Büttner, R., and Zhou, H. (2006). Spatial expression of germ cell markers during maturation of human fetal male gonads: an immunohistochemical study. Hum. Reprod. *21*, 397–404.

Rajpert-De Meyts, E., and Hoei-Hansen, C.E. (2007). From gonocytes to testicular cancer: the role of impaired gonadal development. Ann. NY Acad. Sci. *1120*, 168–180.

Rajpert-De Meyts, E., and Skakkebaek, N.E. (1993). The possible role of sex hormones in the development of testicular cancer. Eur. Urol. *23*, 54–61.

Rajpert-De Meyts, E., Hanstein, R., Jørgensen, N., Graem, N., Vogt, P.H., and Skakkebaek, N.E. (2004). Developmental expression of POU5F1 (OCT-3/4) in normal and dysgenetic human gonads. Hum. Reprod. *19*, 1338–1344.

Rajpert-De Meyts, E., Almstrup, K., and Skakkebaek, N.E. (2013). Testicular dysgenesis syndrome and carcinoma in situ testis. In Atlas on the Human Testis, D. Jezek, ed. (Springer-Verlag), pp. 159–178.

Rajpert-De Meyts, E., McGlynn, K.A., Okamoto, K., Jewett, M.A., and Bokemeyer, C. (2016). Testicular germ cell tumours. Lancet *387*, 1762–1774.

Rotgers, E., Jørgensen, A., and Yao, H.H. (2018). At the crossroads of fate-somatic cell lineage specification in the fetal gonad. Endocr. Rev. *39*, 739–759.

Sinclair, A.H., Berta, P., Palmer, M.S., Hawkins, J.R., Griffiths, B.L., Smith, M.J., Foster, J.W., Frischauf, A.M., Lovell-Badge, R., and Goodfellow, P.N. (1990). A gene from the human sex-determining region encodes a protein with homology to a conserved DNA-binding motif. Nature *346*, 240–244.

Skakkebaek, N.E., Berthelsen, J.G., Giwercman, A., and Müller, J. (1987). Carcinoma-in-situ of the testis: possible origin from gonocytes and precursor of all types of germ cell tumours except spermatocytoma. Int. J. Androl. *10*, 19–28.

Skakkebaek, N.E., Rajpert-De Meyts, E., and Main, K.M. (2001). Testicular dysgenesis syndrome: an increasingly common developmental disorder with environmental aspects. Hum. Reprod. *16*, 972–978.

Skakkebaek, N.E., Rajpert-De Meyts, E., Buck Louis, G.M., Toppari, J., Andersson, A.M., Eisenberg, M.L., Jensen, T.K., Jørgensen, N., Swan, S.H., Sapra, K.J., et al. (2016). Male reproductive disorders and fertility trends: influences of environment and genetic susceptibility. Physiol. Rev. *96*, 55–97.

Søeborg, T., Frederiksen, H., Johannsen, T.H., Andersson, A.M., and Juul, A. (2017). Isotope-dilution TurboFlow-LC-MS/MS method for simultaneous quantification of ten steroid metabolites in serum. Clin. Chim. Acta *468*, 180–186.

Souquet, B., Tourpin, S., Messiaen, S., Moison, D., Habert, R., and Livera, G. (2012). Nodal signaling regulates the entry into meiosis in fetal germ cells. Endocrinology *153*, 2466–2473.

Spiller, C.M., Feng, C.W., Jackson, A., Gillis, A.J., Rolland, A.D., Looijenga, L.H., Koopman, P., and Bowles, J. (2012). Endogenous Nodal signaling regulates germ cell potency during mammalian testis development. Development *139*, 4123–4132.

Spiller, C., Burnet, G., and Bowles, J. (2017). Regulation of fetal male germ cell development by members of the TGFβ superfamily. Stem Cell Res. *24*, 174–180.

van den Driesche, S., McKinnell, C., Calarrão, A., Kennedy, L., Hutchison, G.R., Hrabalkova, L., Jobling, M.S., Macpherson, S., Anderson, R.A., Sharpe, R.M., and Mitchell, R.T. (2015a). Comparative effects of di(n-butyl) phthalate exposure on fetal germ cell development in the rat and in human fetal testis xenografts. Environ. Health Perspect. *123*, 223–230.

van den Driesche, S., Macdonald, J., Anderson, R.A., Johnston, Z.C., Chetty, T., Smith, L.B., Mckinnell, C., Dean, A., Homer, N.Z., Jorgensen, A., et al. (2015b). Prolonged exposure to acetaminophen reduces testosterone production by the human fetal testis in a xenograft model. Sci. Transl. Med. *7*, 288ra80.

Wu, Q., Kanata, K., Saba, R., Deng, C.X., Hamada, H., and Saga, Y. (2013). Nodal/activin signaling promotes male germ cell fate and suppresses female programming in somatic cells. Development *140*, 291–300.

STAR★METHODS

KEY RESOURCES TABLE

REAGENT or RESOURCE	SOURCE	IDENTIFIER
Antibodies		
Mouse monoclonal anti-OCT3/4 (C-10)	Santa Cruz	Sc-5279; RRID: AB_628051
Goat polyclonal anti-NANOG	R&D Systems	AF-1997; RRID: AB_355097
Mouse monoclonal anti-AP2γ (6E4/4)	Santa Cruz	Sc-12762; RRID: AB_667770
Mouse monoclonal anti-SALL4 (EE-30)	Santa Cruz	Sc-101147; RRID: AB_1129262
Goat polyclonal anti-LIN28A	R&D Systems	AF-3757; RRID: AB_2234537
Rabbit polyclonal anti-C-KIT (CD117)	Dako	A4502; RRID: AB_2335702
Mouse monoclonal anti-MAGE-A4	Non-commercial	Gift from Prof. Spagnoli
Goat polyclonal anti-AMH (MIS, C-20)	Santa Cruz	Sc-6886; RRID: AB_649207
Rabbit polyclonal anti-SOX9	Millipore	AB5535; RRID: AB_2239761
Rabbit monoclonal anti-cPARP	Cell Signaling	5625; RRID: AB_10699460
Mouse monoclonal anti-BrdU	Dako	M0744; RRID: AB_10013660
Mouse monoclonal anti-COUP-TFII (H7147)	Perseus Proteomics	PP-H7147-60; RRID: AB_2314222
Rabbit polyclonal anti-CYP11A1	Sigma	HPA016436; RRID: AB_1847423
Mouse monoclonal anti-γH2A.X (phosho S139)(9F3)	Abcam	Ab26350; RRID: AB_470861
Rabbit polyclonal anti-SCP3	Novus	NB300-232; RRID: AB_2087193
Rabbit polyclonal anti-VASA (DDX4)	Abcam	Ab13840; RRID: AB_443012
Rabbit polyclonal anti-FOXL2	Non-commercial	Gift from Prof. Wilhelm
Rabbit polyclonal anti-DMRT1	Sigma	HPA027850; RRID: AB_10600868
Biological Samples		
Human fetal testis and ovary tissue	Copenhagen University Hospital	Department Growth and Reproduction fetal tissue collection. Permit H-1-2012-007
Human fetal testis tissue	Edinburgh University	Centre for Reproductive Health fetal tissue collection. Permit LREC08/S1101/1
Chemicals, Peptides, and Recombinant Proteins		
SB431542	Sigma-Aldrich	S4317
Recombinant Nodal	R&D Systems	3218-ND-025
Recombinant Lefty	R&D Systems	746-LF-025
Recombinant Activin A	R&D Systems	338-AC-010
Recombinant Follistatin	R&D Systems	669-FO-025
Experimental Models: Organisms/Strains		
Male CD1 nude mice	Charles River UK, Margate, England	Crl-CD1-*Foxn1*^{nu}
Oligonucleotides		
See Table S3 for primer details		N/A

CONTACT FOR REAGENT AND RESOURCE SHARING

Further information and requests for resources and reagents should be directed to and will be fulfilled by the Lead Contact, Anne Jørgensen (aj@rh.regionh.dk).

EXPERIMENTAL MODEL AND SUBJECT DETAILS

Collection of human fetal gonads in Denmark

Human fetal gonads were isolated from material available following elective termination of pregnancy during the first trimester at the Department of Gynaecology at Copenhagen University Hospital (Rigshospitalet) and Hvidovre Hospital, Denmark. The regional ethics committee approved this study (permit number H-1-2012-007, including amendments 48801, 50662 and 55184) and women

gave their informed written and oral consent. None of the terminations were for reasons of fetal abnormality and all fetuses appeared morphologically normal. The fetuses were between gestational week (GW) 7 and 12, with fetal age determined by scanning crown-rump length and by evaluation of foot length (Evtouchenko et al., 1996). Fetal testis/mesonephros tissue was dissected in ice-cold PBS and immediately set-up in *ex vivo* cultures. Testis tissue from 54 male fetuses was used for *ex vivo* culture followed by formalin fixation. Tissue from 9 male fetuses were fixed immediately and used as age-matched controls (some of which were also used in a previous study, Jørgensen et al., 2015). Finally, gonads from 11 male and 14 female fetuses were snap-frozen and used for investigation of gene expression. This corresponded to gonadal tissue from 79 fetuses in total.

Collection of human fetal gonads in UK

First-trimester (8-12 GW) and second-trimester (13–20 GW) human fetal testes were obtained following termination of pregnancy. Women gave written informed consent in accordance with national guidelines and ethical approval was obtained from the Lothian Research Ethics Committee (LREC08/S1101/1). No terminations were related to fetal abnormalities. In addition, fetal tissue was provided by the Human Developmental Biology Resource (www.hdbr.org). After dissection, the fetal testis was placed immediately into ice-cold media containing Liebowitz L-15 with glutamine, 10% fetal bovine serum, 1% penicillin/streptomycin and 1% non-essential amino acids (all Sigma, Poole, UK) before *ex vivo* culture and xenografting. Tissue from 3 male 1st trimester and 5 male 2nd trimester fetuses were used for hanging drop *ex vivo* culture followed by xenografting, while 7 testes from 1st trimester and 15 testes from 2nd trimester fetuses were used for gene expression analysis. This corresponded to gonadal tissue from 30 fetuses in total.

Nude mice

Xenografting was performed according to the Animal (Scientific Procedures) Act 1986 following specific approval by UK Home Office and animals were maintained in accordance with UK Home Office guidelines under project license number PPL60/4654. Male CD1-nude mice (aged 6-8 weeks, n = 38, Charles River UK, Margate, England) were used for experiments. Mice received analgesia (Rimadyl LA, Pfizer, NY, USA) and antibiotics (Baytril, Bayer, Germany) in the drinking water for 5 days post-surgery.

METHOD DETAILS

Ex vivo testis tissue culture

Fetal testes were cultured *ex vivo* in hanging drops as described previously with comparison of cultured tissue to pre-culture controls and age-matched control (Jørgensen et al., 2015). In brief, fetal testis tissue (and mesonephros in 1st trimester samples) was cultured in 40 μl medium for 6-14 days. Medium composition was: MEMα media supplemented with 1 × MEM non-essential amino acids (Invitrogen), 2 mM sodium pyruvate, 2 mM L-glutamine, 1 × Insulin, Transferrin and Selenium (ITS) supplement, (Sigma-Aldrich), 1 × Penicillin/Streptomycin, 10% Fetal Bovine Serum (FBS). All cell media and supplements were from GIBCO (Naerum, Denmark), except ITS (Sigma-Aldrich, Broendby, Denmark). Gonads were cultured at 37°C under 5% CO_2 with complete medium change every 48 hr. In general, each testis/mesonephros (1st trimester) and testis (2nd trimester) was divided into approximately 1 mm^3 pieces with at least one piece from each testis used as vehicle control. Tissue fragments were cultured in medium containing the ALK4/5/7 inhibitor SB431542 (20 μM), recombinant Lefty (100 ng/ml), recombinant Nodal (50 ng/ml), recombinant Follistatin (100 ng/ml), recombinant Activin A (50 ng/ml) or vehicle (0.1% DMSO, 0.1% BSA in PBS or 0.1% BSA, 4 mM HCl in PBS). All recombinant proteins were from R&D Systems while SB431542 was from Sigma-Aldrich.

Grafting of human fetal testis tissue into nude mice

Male CD1-nude mice were anesthetized by inhalation of isofluorane, castrated, and small pieces (1 mm^3) of human testis tissue were inserted subcutaneously under the dorsal skin using a 13G cancer implant needle (Popper and Sons, NY, USA) as previously described (van den Driesche et al., 2015b). The human fetal testis tissue pieces had been cultured *ex vivo* for 6 or 10 days with SB431542 (20 μM), Nodal (50 ng/ml) or vehicle control (0.1% DMSO or 0.1% BSA, 4 mM HCl in PBS) prior to grafting. Between two and six testis tissue pieces from a single fetus were inserted on either side of the midline. After the 6 weeks grafting period host mice were killed by cervical dislocation and blood obtained by cardiac puncture for measurement of testosterone. Seminal vesicles were removed and weighed, and xenografts were retrieved and weighed.

Immunohistochemistry

Gonadal tissue was fixed in formalin or Bouins fluid either immediately after dissection (and used as pre-culture or age-matched controls), at the end of the *ex vivo* culture period or after xenografting. The fixed gonads were dehydrated, paraffin embedded and sectioned (4 μm) using standard procedures. Immunohistochemistry was conducted as previously described for formalin fixed samples (Jørgensen et al., 2012). In brief, antigen retrieval was accomplished by microwaving the sections for 15 min in retrieval buffer. Sections were then incubated with 2% non-immune goat serum (Zymed Histostain kit, San Francisco, CA, USA) or 0.5% milk powder diluted in Tris buffered saline (TBS) to minimize cross-reactivity. Primary antibodies, dilutions, and retrieval buffers are listed in Table S1. After 16 h of incubation at 4°C and 1 h at room temperature, the sections were incubated with biotinylated goat anti-rabbit

IgG (Zymed Histostain kit) or biotinylated goat anti-mouse IgG (1:400), before a peroxidase-conjugated streptavidin complex (Zymed Histostain kit) was used as a tertiary layer. Visualization was performed with amino ethyl carbasole (AEC) (Invitrogen by Life Technology, Frederick, MD, USA) yielding a red color and sections were counterstained with Mayer's hematoxylin. Immunohistochemistry on Bouin's fluid fixed samples was conducted as previously described (Mitchell et al., 2010). In brief, sections (4 μm) were subjected to heat-induced antigen retrieval in 0.01 M citrate buffer (pH 6) in a pressure cooker and endogenous peroxidase was blocked with 3% (v/v) H_2O_2 in methanol for 30 min. Between each step, sections were washed in Tris-buffered saline (TBS). Sections were incubated in appropriate normal serum diluted 1:5 with TBS containing 5% (w/v) bovine serum albumin (BSA) for 30 min. Sections were incubated overnight with primary antibody diluted in serum at 4°C in a humidified chamber and then incubated for 30 min with the appropriate ImmPRESS HRP (peroxidase) secondary antibody, diluted in normal serum. Visualization was performed using ImmPACT DAB peroxidase (HRP) substrate (Vector Laboratories) yielding a brown color and sections were counterstained with Meyer's hematoxylin before mounting with Aquatex (Merck, Damstadt, Germany). For both protocols negative controls were included and processed with the primary antibody replaced by the dilution buffer alone. None of the negative control slides showed staining. All sections were initially evaluated on a Nikon Microphot-FXA microscope and then by scanning slides on a NanoZoomer 2.0 HT (Hamamatsu Photonics, Herrsching am Ammersee, Germany) followed by analysis using the software NDPview version 1.2.36 (Hamamatsu Photonics).

Immunofluorescence

Immunofluorescence was performed with Tris-buffered saline (TBS) washes (3 × 5 min) between each step and all incubations were carried out in in a humidity box (Fisher Scientific, UK). Sections (4 μm) were dewaxed and rehydrated using standard procedures, followed by heat-induced antigen retrieval (pressure cooker) in 0.01 M citrate buffer (pH 6) and peroxidase block in 3% (v/v) H_2O_2 in methanol for 30 min. Next, the sections were blocked in normal chicken serum (NCS; Biosera, Ringmer, UK) diluted 1:5 in TBS containing 5% (w/v) BSA (NCS/TBS/BSA), followed by incubation with OCT4 antibody diluted 1:100 in NCS/TBS/BSA overnight at 4°C. The next day, sections were incubated with peroxidase-conjugated chicken anti-mouse secondary antibody (Santa Cruz), diluted 1:200 in NCS/TBS/BSA for 30 min at room temperature (RT), and followed by incubation with Tyr-Cy3 (Perkin Elmer-TSA-Plus Cyanine3 System; Perkin Elmer Life Sciences, Boston, MA, USA) according to manufacturer's instructions. Before the next primary antibody dilution was added, the sections were again subjected to antigen retrieval by blocking in NCS/TBS/BSA and overnight incubation at 4°C with MAGE-A4 antibody diluted 1:200 in NCS/TBS/BSA. On the third day, slides were incubated with peroxidase-conjugated chicken anti-mouse secondary antibody (Santa Cruz) diluted 1:200 in NCS/TBS/BSA for 30 min at RT, followed by incubation with Tyr-Fluorescein (Perkin Elmer-TSA-Plus Fluorescein System; Perkin Elmer Life Sciences) according to manufacturer's instructions. Sections were again subjected to antigen retrieval followed by blocking in NCS/TBS/BSA and incubation with SOX9 antibody diluted 1:2500 in NCS/TBS/BSA overnight at 4°C. Sections were then incubated with peroxidase-conjugated chicken anti-rabbit secondary antibody (Santa Cruz), diluted 1:200 in NCS/TBS/BSA for 30 min at RT, followed by incubation with Tyr-Cy5 (Perkin Elmer-TSA-Plus Cyanine5 System; Perkin Elmer Life Sciences, Boston, MA, USA) according to manufacturer's instructions. Sections were counterstained with DAPI (Sigma) diluted 1:500 in TBS for 10 min. Finally, slides were mounted with Permafluor (Thermo Scientific, UK) and fluorescent images captured using an Olympus BX61 microscope (Olympus).

BrdU incorporation

BrdU incorporation was used to determine the presence of proliferating germ cells just prior to the end of the *ex vivo* culture period as previously described (Jørgensen et al., 2014; Jørgensen et al., 2015). In brief, BrdU labeling reagent (Life Technologies, Naerum, Denmark) was diluted 1:100 in culture media and tissue fragments were placed in BrdU containing media for 6 hr. Tissue pieces were then washed 2 times in PBS for 5 min followed by fixation and paraffin embedding as described above. BrdU was visualized by immunohistochemistry using a BrdU antibody (Table S1) as described in the Immunohistochemistry section, with positively stained cells considered as proliferating.

Quantification of germ cells

To evaluate the IHC staining quantitatively, the number of stained cells per area of tissue was counted. For each sample the entire tissue section was counted. The area was measured using NDPview software (Hamamatsu Photonics, Herrsching am Ammersee, Germany). Germ cells were identified based on OCT4 staining (gonocytes) and MAGE-A4 staining (pre-spermatogonia). Two investigators (AJø and JEN) evaluated all stainings.

TUNEL assay

Apoptosis/DNA fragmentation was detected using the terminal deoxynucleotidyl transferase (TdT)-mediated dNTP nick end labeling (TUNEL) assay (Trevigen, Gaithersburg, MD, USA). A slightly modified version of the manufacturers protocol was applied, using AEC instead of DAB. Sections were counterstained by brief immersion in Mayer's hematoxylin. Positive controls were incubated with TACS nuclease for 1.5 h at 37°C to induce DNA strand breaks. Negative controls were incubated without TdT enzyme.

Quantification of testosterone in mice

Plasma testosterone levels in xenografted host mice were measured at termination by competitive radioimmunoassay using an extraction-based in-house radioimmunoassay method described previously (Corker and Davidson 1978). Testosterone levels were expressed as ng/ml and all samples analyzed in a single assay with three replicates. The detection limit was 45 pg/ml, and the intra-assay coefficient of variation was 8%.

Steroid hormone measurements in culture medium

Analysis of androgen and corticosteroid levels in culture media from *ex vivo* culture was measured by a new and sensitive isotope-dilution TurboFlow-LC-MS/MS method for simultaneous quantification of dehydroepiandrosterone sulfate (DHEAS), Δ4-androstenedione, testosterone, 17α-hydroxyprogesterone (17-OHP), progesterone, 11-deoxycortisol, cortisol, cortisone, corticosterone, and estrone-sulfate (Søeborg et al., 2017). The following modifications were applied: calibration curves were prepared in culture media, control samples were prepared by spiking with high and low concentration of steroids, and all collected media samples were diluted four times in culture media prior to analysis. A few samples were reanalyzed for testosterone after additional sample dilution. Samples were analyzed in 11 batches during summer/autumn of 2016. Each batch included standards for calibration curves, ~20 unknown samples, one blank and three pooled controls spiked with steroid standards at low and high levels. The inter-day variation, expressed as the relative standard deviation (RSD) was $\leq$ 6% for all analytes at both spike levels except for (E1-S) in low spike level (22%). The recovery was > 92% for all analytes at both spike levels. Additional details in Table S2.

AMH measurements in culture medium

AMH levels in culture media from *ex vivo* culture was measured by ELISA using the Beckman Coulter enzyme immunometric assay Reagents Kit (Ref. B13127, lot no. 871046) and Calibrator kit (Ref. B13128, lot no. 789308) according to the manufacturers instruction, except that the lyophilized calibrators were reconstituted in culture media instead of water. Collected media samples were diluted 1:10 in culture media prior to analysis, with additional sample dilution (1:20 and 1:50) necessary for approximately 40% and 10% of the samples, respectively. The detection limit of the AMH assay was 0.14 pmol/L and the inter-assay variation was < 7.5% in the total measurement range.

Quantitative RT-PCR

Quantitative PCR was conducted using the Mx300P platform (Stratagene, Cedar Creek, TX, USA), as previously described (Jørgensen et al., 2013) or the ABI 7900HT (Applied Biosystems). Gene expression was examined using specific primers (Table S3) that were designed to span intron–exon boundaries and all amplicons were sequenced to verify specificity (Eurofins Genomics, Ebersberg, Germany). Standard curve analysis and efficiency of amplification was established to confirm that slopes of the standard curves were close to −3.3 (equivalent to 100% PCR efficiency or two-fold amplification per cycle). Changes in gene expression were quantified using the $2^{-\Delta\Delta Ct}$ method. Expression levels were normalized to *RPS29* expression and calculated as a ratio with fetal testes from GW 7–9 set to 1.

QUANTIFICATION AND STATISTICAL ANALYSIS

Statistical significance was determined using GraphPad Prism Software. Data are presented as mean ± SEM. For cultured samples Student's paired (two-tailed) t test was used. If samples were not paired (Figure S1) Student's unpaired (two-tailed) t test was used. Asterisks indicate statistical significance with * $p < 0.05$, ** $p < 0.01$, *** $p < 0.001$. The number of replicates in each experimental setting and statistical significance are specified in each figure legend.